Supplementary information

Supplementary Figure S1.

The grid coverage (electrodes shown in green), surface potential maps (negativity in blue and positivity in red) and source reconstruction images from 20 subjects (10-10 grids over lateral surfaces of the right and left hemispheres, respectively) are shown in the following images. Both S1 and DW (difference wave: S1-S2) data are present.

Only data from grids with a sufficient number of electrodes (minimum 64 electrodes) were used for source localization. There were 20 subjects with this arrangement. CURRY software (Neuroscan, Compumedics Ltd.) was used for head modeling and source estimation. The sensor 3D positions were extracted from grids in post-implantation MRIs via identification of four corner electrodes and subsequent linear interpolation of electrode positions for the full array. To allow extended current patterns to be mapped, a weighted minimum-norm technique (LORETA: low resolution electromagnetic tomography) was used to estimate current density distributions from S1 signal P50 potentials and so-called difference waves (S1-S2). LORETA solution is based in the assumption of neighboring sources having similar strengths and allows reconstruction of smooth current distributions. Individual BEM (boundary element model) head models were created from the subjects' MRI data and used to solve the forward problem.

Segmentation of the MRI data was performed in order to obtain the boundaries on the surface of the brain and inner skull that enclose tissue compartments which are assumed to be homogeneous and isotropic, with known conductivity values (0.33 and 1.79 S/m, respectively). This involved a routine of realistic head modeling in Curry software via high resolution discretisation of the surfaces with approximately 3500 nodes (about 2000 nodes representing the innermost brain compartment and about 1500 nodes for the CSF's BEM surface). As part of the distributed current density reconstructions with LORETA, the source locations were defined in the cortical surface (source space included thousands of locations and was defined by a sufficiently high sampling of the segmented cortical surface). A rotating source type was used instead of fixed source orientations (i.e. cortical surface normals) in order to allow estimation of omnidirectional currents and minimize the effects of nonoptimal surface segmentations. Noise level in the evoked responses was estimated from the pre-stimulus interval (-100 to 0 ms). Current density regularization parameter lambda (controlling the trade-off between data and the model) was optimized so that the residual deviation equaled 1/SNR (signal-to-noise ratio).

The optimal head modeling for intracranial data is still a matter of research. The use of a single-compartment BEM model has been preferred in conjunction with a spatially smoothed source space in order to avoid the issue of whether grid cortical recordings allow one to reliably define source depth. However, if the latter is true, it is unclear what source localization would provide in addition to cortical surface potential maps. Here, we used a two-compartment BEM model including the innermost brain and cerebrospinal fluid (CSF) compartments.

The main purpose of source localization from grid electrodes was to show differences in terms of individual regions that are involved in both or predominantly in one of two studied processes such as stimulus registration during P50 phase and repetition suppression.

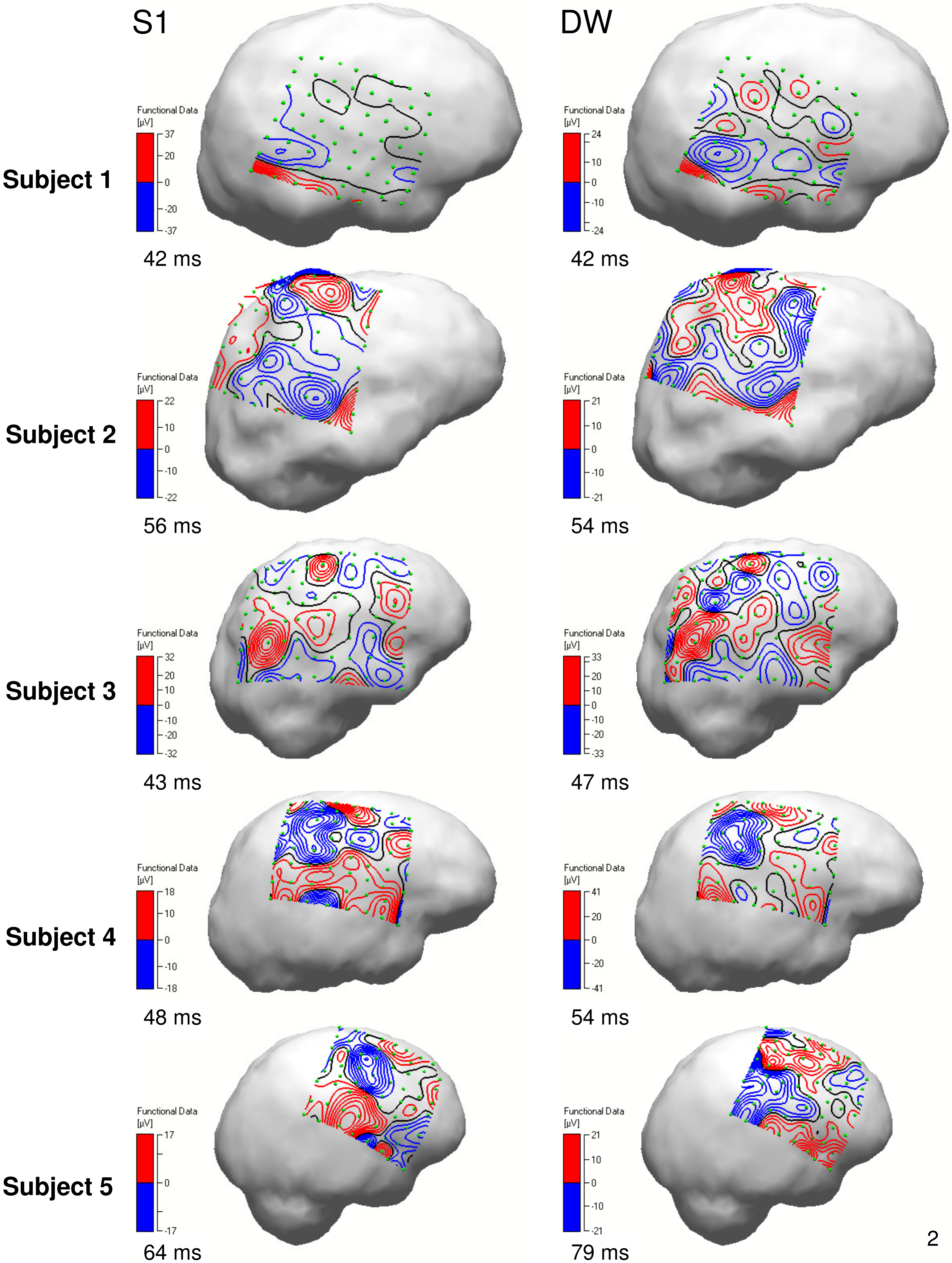
S1
DW
Subject 1
Functional Data [µV]
37 20 0 -20 -37
42 ms
Functional Data [µV]
24 10 0 -10 -24
42 ms
Subject 2
Functional Data [µV]
22 10 0 -10 -22
56 ms
Functional Data [µV]
21 10 0 -10 -21
54 ms
Subject 3
Functional Data [µV]
32 20 10 0 -10 -20 -32
43 ms
Functional Data [µV]
33 20 10 0 -10 -20 -33
47 ms
Subject 4
Functional Data [µV]
18 10 0 -10 -18
48 ms
Functional Data [µV]
41 20 0 -20 -41
54 ms
Subject 5
Functional Data [µV]
17 0 -17
64 ms
Functional Data [µV]
21 10 0 -10 -21
79 ms

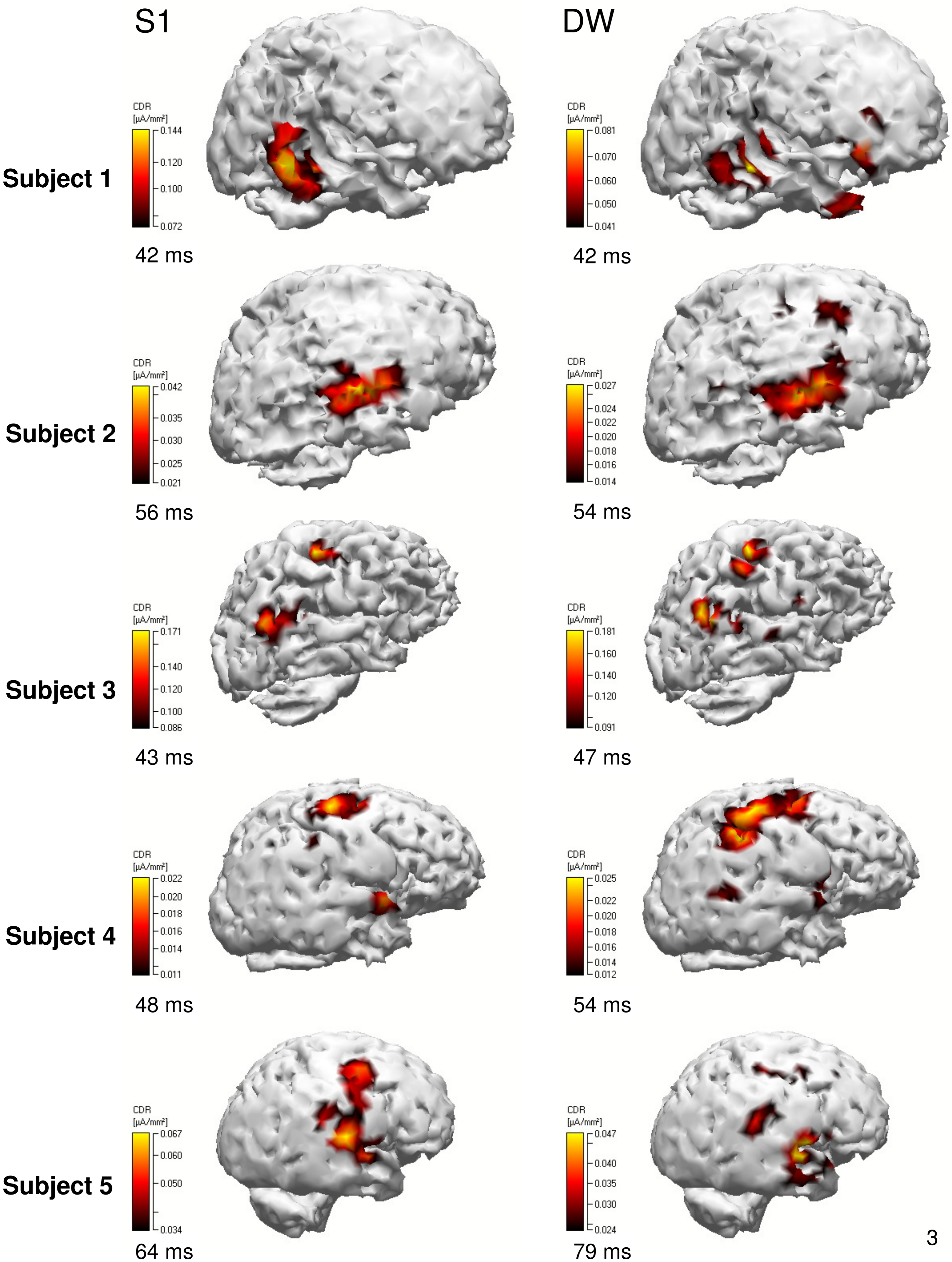
S1
DW
Subject 1
Subject 2
Subject 3
Subject 4
Subject 5
CDR [μA/mm²]
0.144
0.120
0.100
0.072
42 ms
0.081
0.070
0.060
0.050
0.041
42 ms
0.042
0.035
0.030
0.025
0.021
56 ms
0.027
0.024
0.022
0.020
0.018
0.016
0.014
54 ms
0.171
0.140
0.120
0.100
0.086
43 ms
0.181
0.160
0.140
0.120
0.091
47 ms
0.022
0.020
0.018
0.016
0.014
0.011
48 ms
0.025
0.022
0.020
0.018
0.016
0.014
0.012
54 ms
0.067
0.060
0.050
0.034
64 ms
0.047
0.040
0.035
0.030
0.024
79 ms

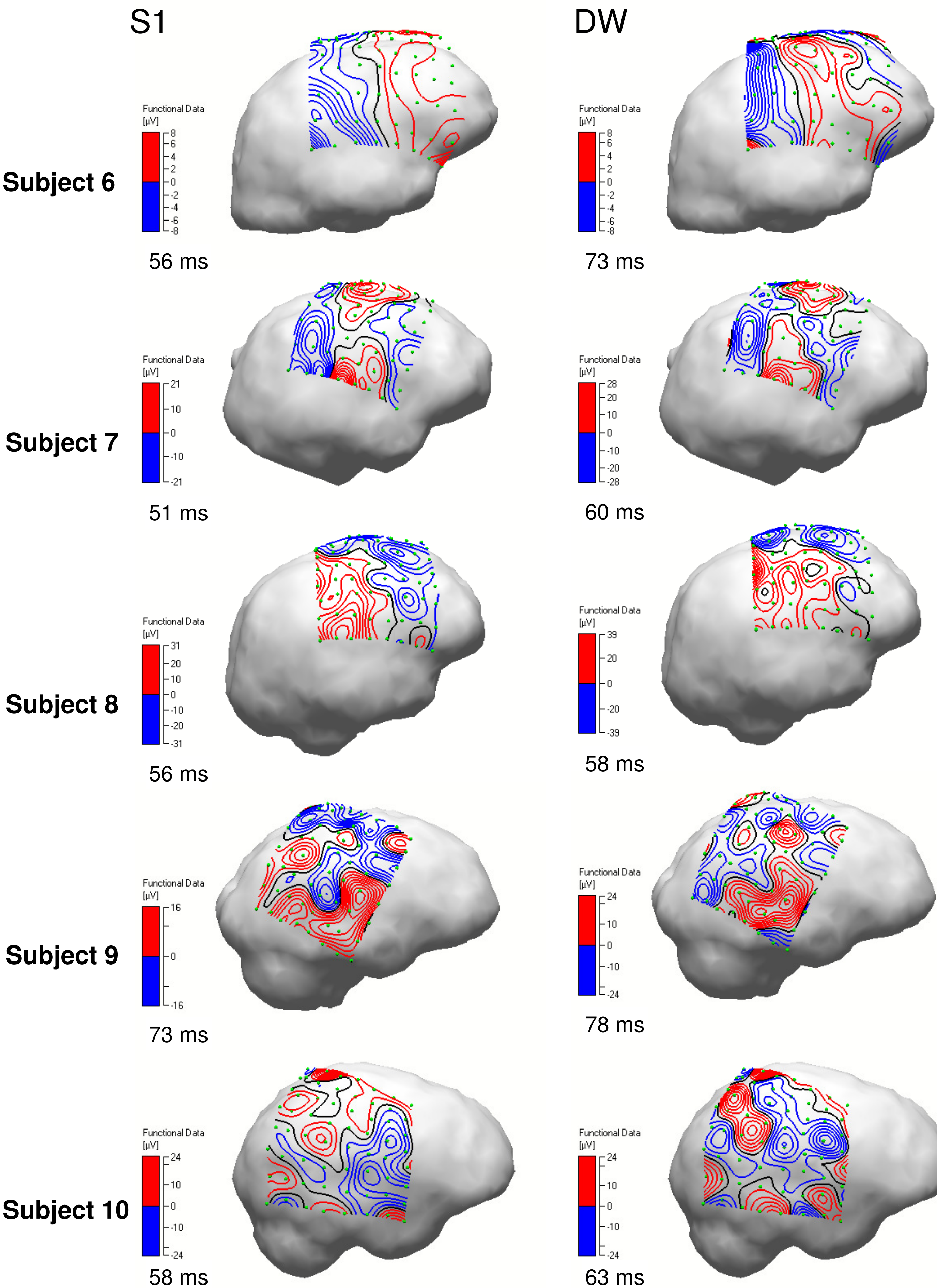
S1
DW
Subject 6
Functional Data [µV]
8 6 4 2 0 -2 -4 -6 -8
56 ms
73 ms
Subject 7
21 10 0 -10 -21
51 ms
28 20 10 0 -10 -20 -28
60 ms
Subject 8
31 20 10 0 -10 -20 -31
56 ms
39 20 0 -20 -39
58 ms
Subject 9
16 0 -16
73 ms
24 10 0 -10 -24
78 ms
Subject 10
24 10 0 -10 -24
58 ms
63 ms

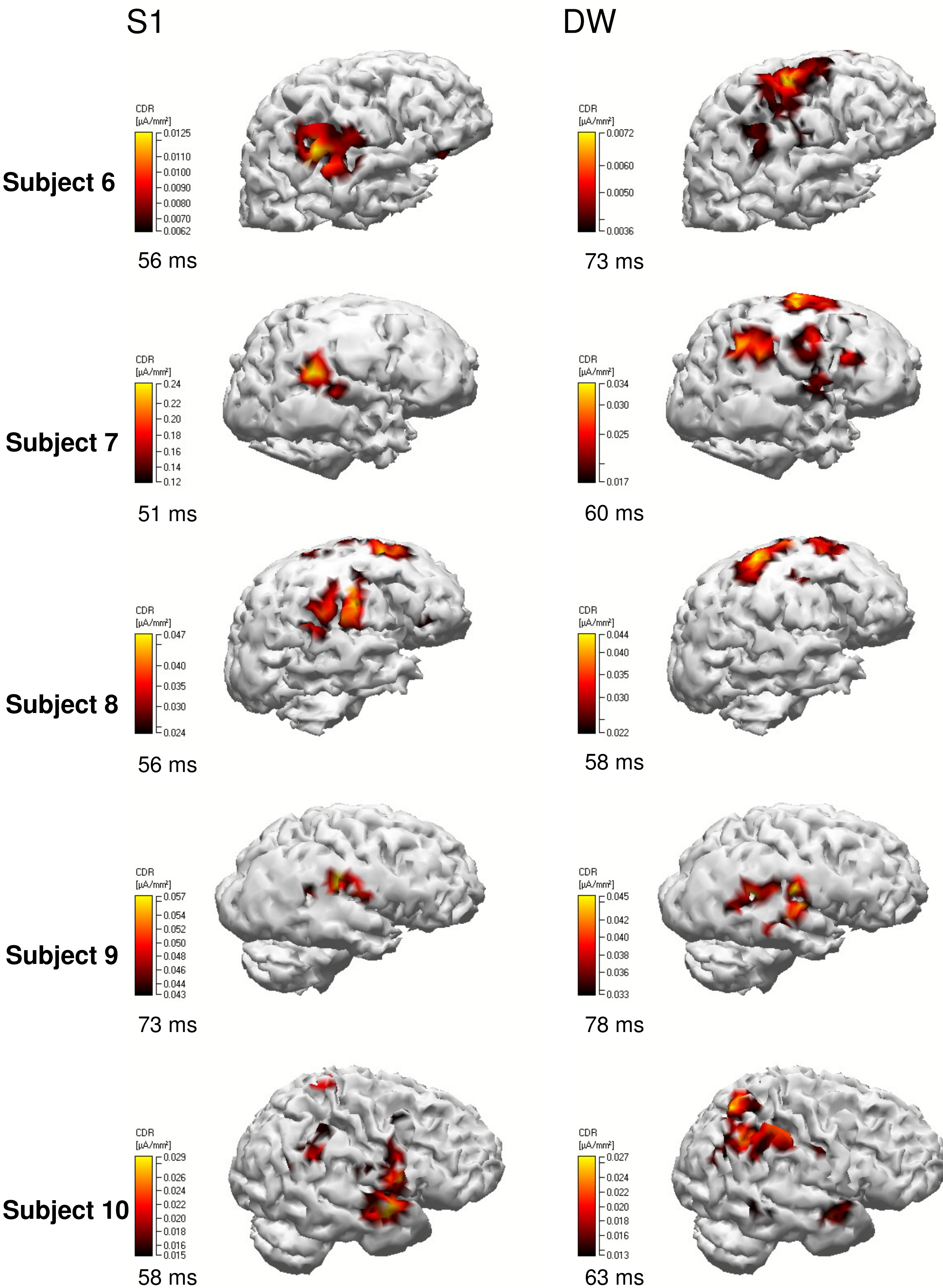
S1
DW
Subject 6
CDR [μA/mm²]
0.0125 0.0110 0.0100 0.0090 0.0080 0.0070 0.0062
56 ms
CDR [μA/mm²]
0.0072 0.0060 0.0050 0.0036
73 ms
Subject 7
CDR [μA/mm²]
0.24 0.22 0.20 0.18 0.16 0.14 0.12
51 ms
CDR [μA/mm²]
0.034 0.030 0.025 0.017
60 ms
Subject 8
CDR [μA/mm²]
0.047 0.040 0.035 0.030 0.024
56 ms
CDR [μA/mm²]
0.044 0.040 0.035 0.030 0.022
58 ms
Subject 9
CDR [μA/mm²]
0.057 0.054 0.052 0.050 0.048 0.046 0.044 0.043
73 ms
CDR [μA/mm²]
0.045 0.042 0.040 0.038 0.036 0.033
78 ms
Subject 10
CDR [μA/mm²]
0.029 0.026 0.024 0.022 0.020 0.018 0.016 0.015
58 ms
CDR [μA/mm²]
0.027 0.024 0.022 0.020 0.018 0.016 0.013
63 ms

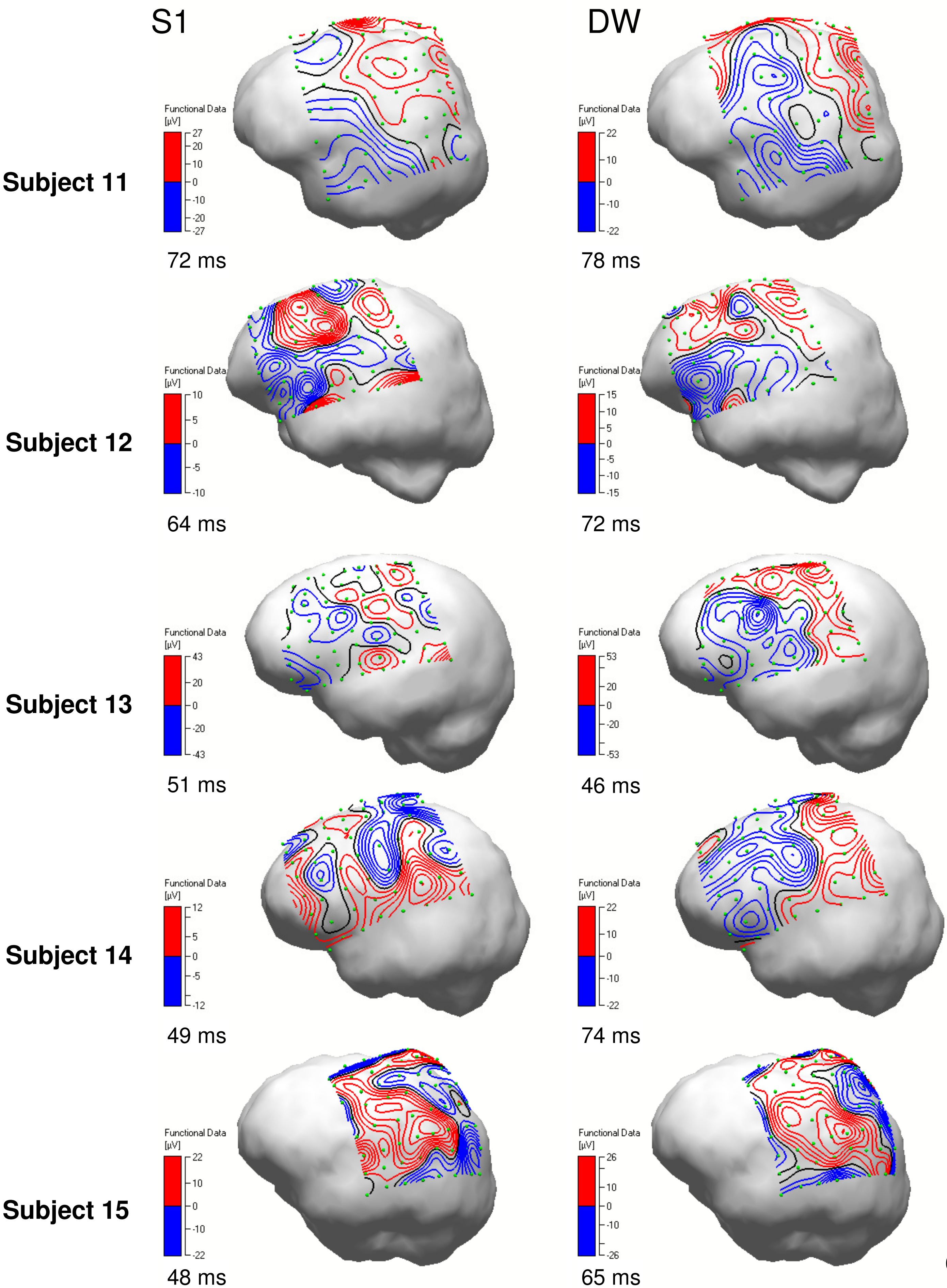
S1
DW
Subject 11
Functional Data [µV]
27 20 10 0 -10 -20 -27
72 ms
Functional Data [µV]
22 10 0 -10 -22
78 ms
Subject 12
Functional Data [µV]
10 5 0 -5 -10
64 ms
Functional Data [µV]
15 10 5 0 -5 -10 -15
72 ms
Subject 13
Functional Data [µV]
43 20 0 -20 -43
51 ms
Functional Data [µV]
53 20 0 -20 -53
46 ms
Subject 14
Functional Data [µV]
12 5 0 -5 -12
49 ms
Functional Data [µV]
22 10 0 -10 -22
74 ms
Subject 15
Functional Data [µV]
22 10 0 -10 -22
48 ms
Functional Data [µV]
26 10 0 -10 -26
65 ms

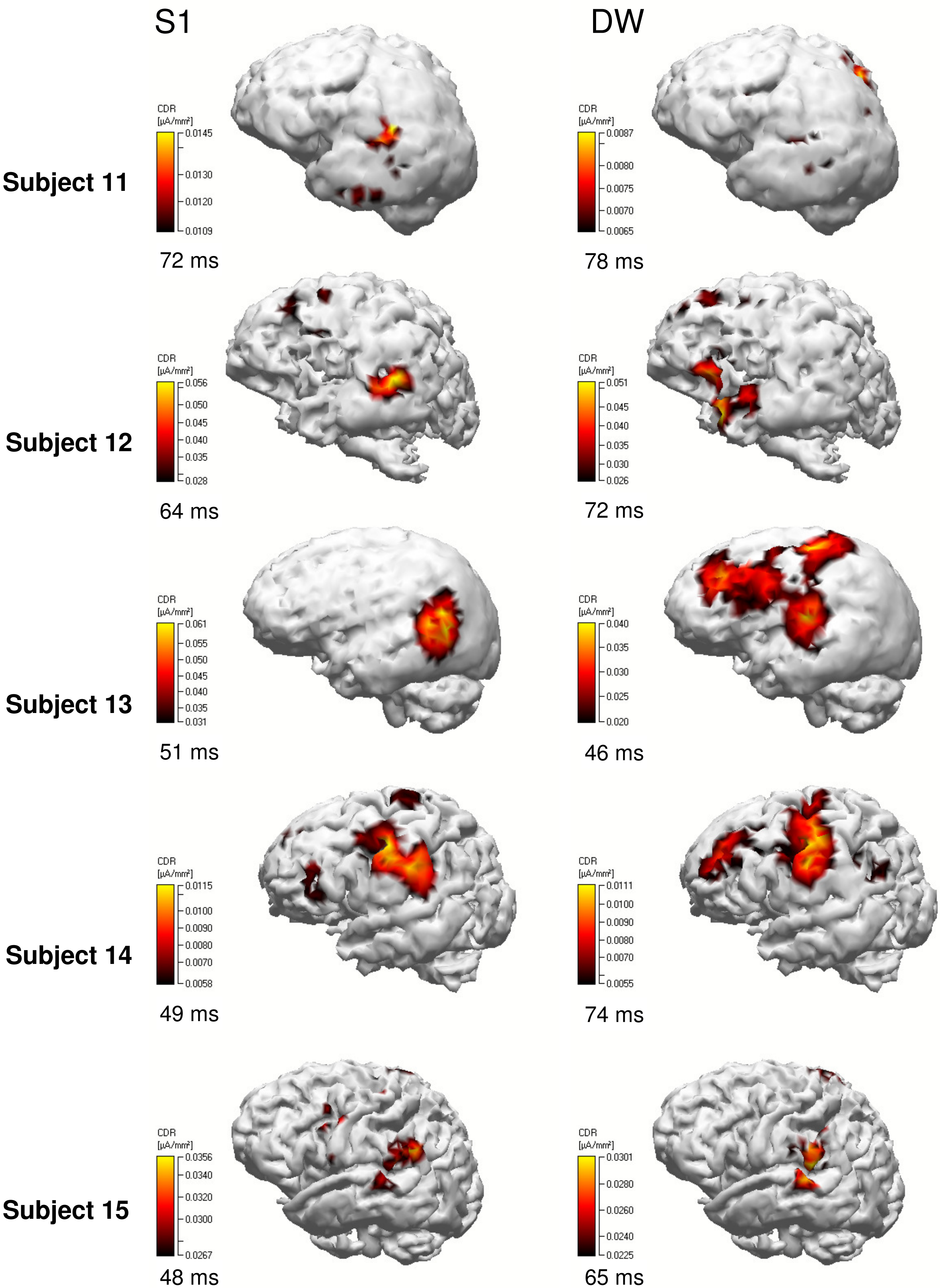
S1
DW
Subject 11
CDR [μA/mm²]
0.0145
0.0130
0.0120
0.0109
72 ms
CDR [μA/mm²]
0.0087
0.0080
0.0075
0.0070
0.0065
78 ms
Subject 12
CDR [μA/mm²]
0.056
0.050
0.045
0.040
0.035
0.028
64 ms
CDR [μA/mm²]
0.051
0.045
0.040
0.035
0.030
0.026
72 ms
Subject 13
CDR [μA/mm²]
0.061
0.055
0.050
0.045
0.040
0.035
0.031
51 ms
CDR [μA/mm²]
0.040
0.035
0.030
0.025
0.020
46 ms
Subject 14
CDR [μA/mm²]
0.0115
0.0100
0.0090
0.0080
0.0070
0.0058
49 ms
CDR [μA/mm²]
0.0111
0.0100
0.0090
0.0080
0.0070
0.0055
74 ms
Subject 15
CDR [μA/mm²]
0.0356
0.0340
0.0320
0.0300
0.0267
48 ms
CDR [μA/mm²]
0.0301
0.0280
0.0260
0.0240
0.0225
65 ms

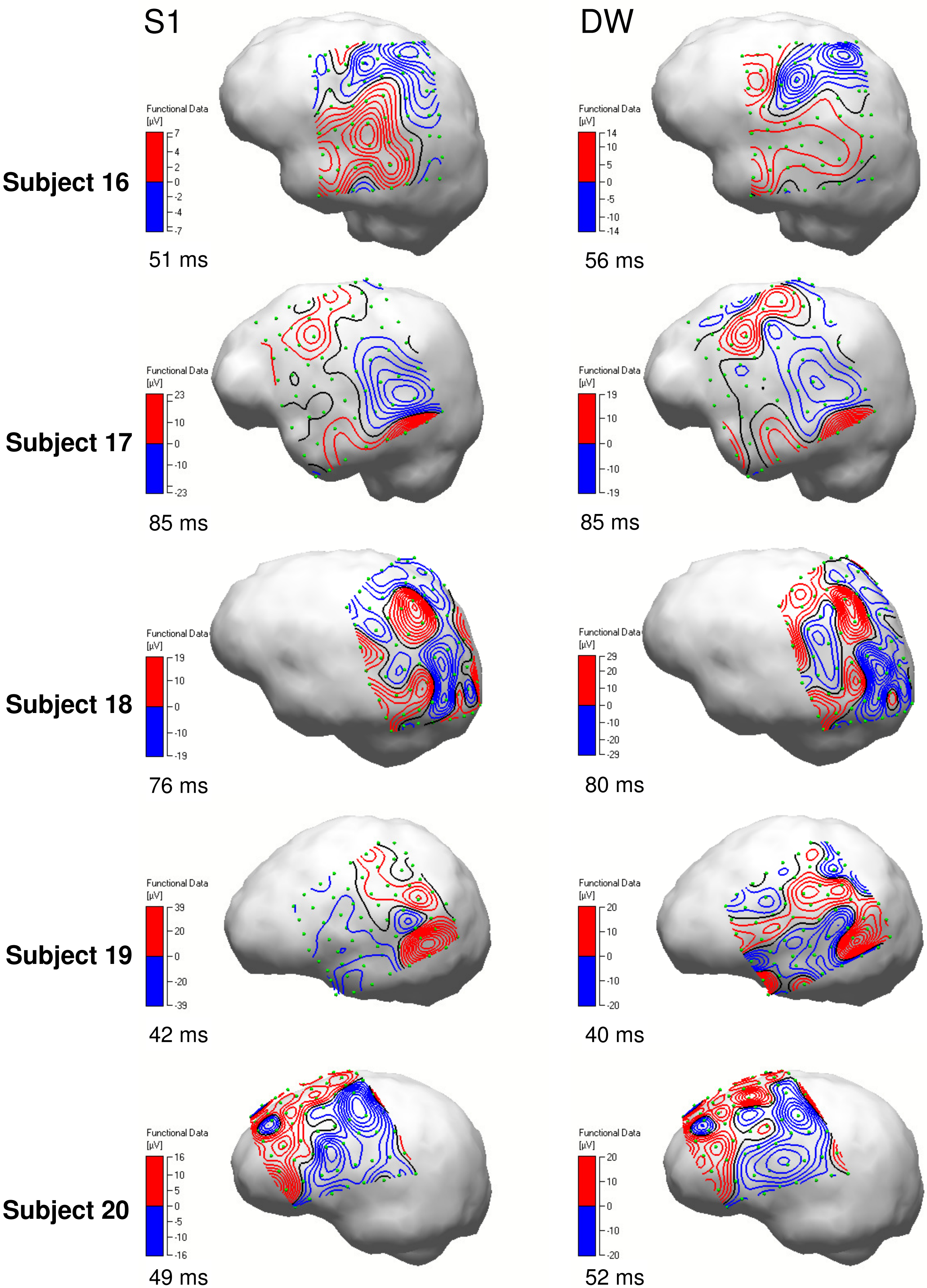
S1
DW
Subject 16
Functional Data [µV]
7 4 2 0 -2 -4 -7
51 ms
Functional Data [µV]
14 10 5 0 -5 -10 -14
56 ms
Subject 17
Functional Data [µV]
23 10 0 -10 -23
85 ms
Functional Data [µV]
19 10 0 -10 -19
85 ms
Subject 18
Functional Data [µV]
19 10 0 -10 -19
76 ms
Functional Data [µV]
29 20 10 0 -10 -20 -29
80 ms
Subject 19
Functional Data [µV]
39 20 0 -20 -39
42 ms
Functional Data [µV]
20 10 0 -10 -20
40 ms
Subject 20
Functional Data [µV]
16 10 5 0 -5 -10 -16
49 ms
Functional Data [µV]
20 10 0 -10 -20
52 ms

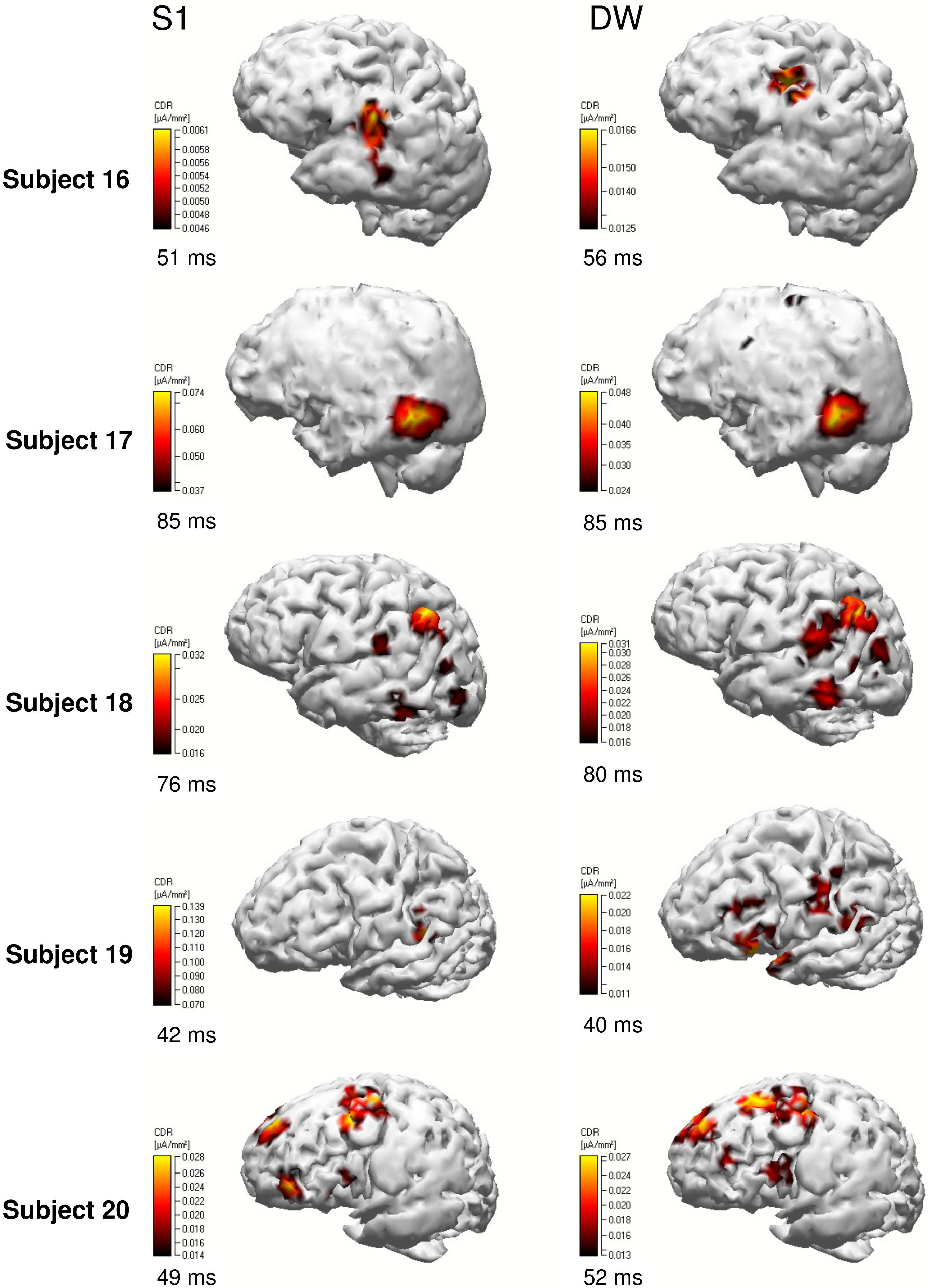
S1
DW
Subject 16
CDR [μA/mm²]
0.0061 0.0058 0.0056 0.0054 0.0052 0.0050 0.0048 0.0046
51 ms
CDR [μA/mm²]
0.0166 0.0150 0.0140 0.0125
56 ms
Subject 17
CDR [μA/mm²]
0.074 0.060 0.050 0.037
85 ms
CDR [μA/mm²]
0.048 0.040 0.035 0.030 0.024
85 ms
Subject 18
CDR [μA/mm²]
0.032 0.025 0.020 0.016
76 ms
CDR [μA/mm²]
0.031 0.030 0.028 0.026 0.024 0.022 0.020 0.018 0.016
80 ms
Subject 19
CDR [μA/mm²]
0.139 0.130 0.120 0.110 0.100 0.090 0.080 0.070
42 ms
CDR [μA/mm²]
0.022 0.020 0.018 0.016 0.014 0.011
40 ms
Subject 20
CDR [μA/mm²]
0.028 0.026 0.024 0.022 0.020 0.018 0.016 0.014
49 ms
CDR [μA/mm²]
0.027 0.024 0.022 0.020 0.018 0.016 0.013
52 ms